



**HAL**  
open science

# Analytical Behavior Law for a Constant Pitch Conical Compression Spring

Manuel Paredes, Emmanuel Rodriguez, Marc Sartor

► **To cite this version:**

Manuel Paredes, Emmanuel Rodriguez, Marc Sartor. Analytical Behavior Law for a Constant Pitch Conical Compression Spring. *Journal of Mechanical Design*, 2006, 128 (6), 10.1115/1.2338580 . hal-01878088

**HAL Id: hal-01878088**

**<https://insa-toulouse.hal.science/hal-01878088v1>**

Submitted on 20 Sep 2018

**HAL** is a multi-disciplinary open access archive for the deposit and dissemination of scientific research documents, whether they are published or not. The documents may come from teaching and research institutions in France or abroad, or from public or private research centers.

L'archive ouverte pluridisciplinaire **HAL**, est destinée au dépôt et à la diffusion de documents scientifiques de niveau recherche, publiés ou non, émanant des établissements d'enseignement et de recherche français ou étrangers, des laboratoires publics ou privés.

# Analytical Behavior Law for a Constant Pitch Conical Compression Spring

## Authors:

Emmanuel Rodriguez, Manuel Paredes, Marc Sartor

Laboratoire de Génie Mécanique de Toulouse, INSA, 135 avenue de Rangueil, F-31077 Toulouse,  
France, phone: +33 5 61 55 98 93, fax: +33 5 61 55 97 00, emmanuel.rodriguez@insa-toulouse.fr

## Abstract:

**Background.** Cylindrical compression spring behavior has been described in the literature using an efficient analytical model. Conical compression spring behavior has a linear phase but can also have a non-linear phase. The rate of the linear phase can easily be calculated but no analytical model exists to describe the non-linear phase precisely. The non-linear phase can only be determined by a discretizing algorithm.

**Method of Approach.** This paper presents, for the first time, analytical continuous expressions of length as a function of load and load as a function of length for a constant pitch conical compression spring, in linear and non-linear phases. The method leading to the first above analytical expression involves separating free and solid/ground coils, and integrating elementary deflections along the whole spring. The inverse process to obtain the spring load from its length is assimilated to solve a fourth order polynomial.

**Results.** Two analytical models are obtained. One to determine the Length vs. Load curve and the other for the Load vs. Length curve. Validation of the new conical spring models in comparison with experimental data is performed. An example of an application with the new models is also provided.

**Conclusion:** The behavior law of a conical compression spring can now be analytically determined. This kind of formula is useful for designers who seek to avoid using tedious algorithms. Analytical models can also be useful in developing assistance tools for conical spring design, especially where optimization methods are used.

**Keywords:** constant pitch conical spring, analytical models, linear, non-linear, fourth order polynomial, design optimization.

## 1 Introduction

Helical springs are among the most widespread components in mechanical systems. Wahl [1] summarized basic and essential definitions, characteristics, behavior models and calculation methods relating to the main types of springs. More recently, in order to provide precise spring applications, mechanical design research has been conducted leading to significant improvements in knowledge of springs. Ding and Selig [2] proposed a new compression spring model based on its compliance matrix. The model goes beyond the standard Euler-Bernoulli beam theory that induces the “closely coiled spring approximation”, hence allowing for larger deflections. Becker, Chassie and Cleghorn investigated buckling of helical compression springs [3] and their resonant frequencies under static axial load with clamped ends [4]. Jiang and Henshall [5] developed an efficient finite element model for helical springs. Todinov [6] studied fatigue crack origin of compression springs through analysis of the maximum principle tensile stress location and effects of shot-peening.

Conical springs provide a commonly used solution for applications with constraints of reduced length or space. They can be used in many different mechanisms, as with contactors and switches in the electrical field. Indeed they are often chosen for one special characteristic, i.e. their ability to telescope, meaning they take up very little space at maximum compression while storing as much energy as cylindrical springs. But conical springs also have other specific features. For example, their load-length characteristics are usually non-linear. Wahl [1] did not mention these springs. However, there has been research into conical springs. The Institute of Spring Technology [7] proposes definitions and calculations for conical spring general characteristics such as the spring rate in its linear range. In parallel with this work, in order to improve our knowledge of conical springs and describe their behavior in greater detail, research has been performed into their fundamental frequencies [8-10], buckling [11] and lateral loading [12]. Until now, the IST conical spring calculation model has provided non-linear load-length characteristics from an incremental algorithm [7]. This involves a process that discretizes each coil to evaluate deflection as a function of load. This necessarily leads to an approximated load-length relation. This algorithm is non-inversible since it calculates spring deflection from any load value, but cannot directly evaluate load from a deflection value. The ‘Advanced Spring Design 6’ software from the Spring Manufacturers Institute [13] and Universal Technical Systems [14] provides a simple and complete interface. It offers design verification, but simplifies conical spring behavior into a linear phenomenon. The ‘Spring Design and Validation 7’ software from IST [15] verifies the accuracy of a conical spring configuration, taking into account its non-linear characteristic, but is unable to offer conical spring design in accordance with the designer’s needs, as a synthesis tool.

Numerical optimization methods can be used to define such a tool. Such methods have already allowed for interesting improvements in mechanical component design. Stochastic methods such as genetic algorithms have also often been applied. Yoshimura et al. [16] developed a multi-objective method to optimize multiple cross-sectional shapes for automotive body frames. Lyu et al. [17] proposed a method to design multi-component structural assemblies. Giassi et al. [18] developed a method based on a genetic algorithm to optimize a hull-shape aimed at minimizing the resistance and energy created by a ship's displacement. Non-linear mathematical programming methods have also often been used. Maddisetty and Frecker [19] optimized the topology of compliant mechanics and piezoceramic actuators using the Sequential Linear Programming method. Sandgren [20] proposed an optimization method adapted to mechanical design problems with non-linear integer or discrete variables and also devised an application for simplified spring design. In order to manage discrete variables, a 'branch and bound' procedure is used. In previous works, we developed design assistance tools for compression [21] and extension [22] cylindrical springs. In our approach, the designer defines his need using a user-friendly interface and the tool applies numerical optimization methods to directly propose the optimum design to respond to requirements. Such a synthesis tool for conical springs responds to designer demands, since it would be a great help in defining and checking any conical spring. In tackling the development of an optimal design tool for conical springs, we had to face the lack of a precise and invertible analytical expression for the load-length law. Indeed, numerical optimization methods are more likely to be efficient when the behavior of the component under study is described analytically. Wu and Hsu [23] developed an analytical model for a particular type of conical spring. Their study focuses on a conical spring with a constant helix angle, that does not telescope, and has cylindrical closed and ground ends. This model is based on a separating analysis between free coils and solid/ground ones, and gives spring deflection as a function of load. The result is approximated in a third order polynomial for a dynamic study. This study is thus not applicable for common conical springs with constant pitch. Rather, the paper sets forth the analytical expressions we propose to use to describe the behavior of a constant pitch conical spring.

Firstly, conical spring characteristics are presented as the basis of further developments. Then the first expression – length as a function of load – is described, and determination of the second 'inverse' expression – load as a function of length – is explained. We go on to show how these models have been validated by experimentation. Finally, an illustrative example using new models is proposed.

The use of these two load-length relations within an optimization method will be further developed in future works.

## 2 Conical spring characteristics

**2.1 Parameters of a constant pitch conical spring.** A conical compression spring with constant pitch and circular wire, is studied. Its design is fully defined by six parameters (see Fig. 1).

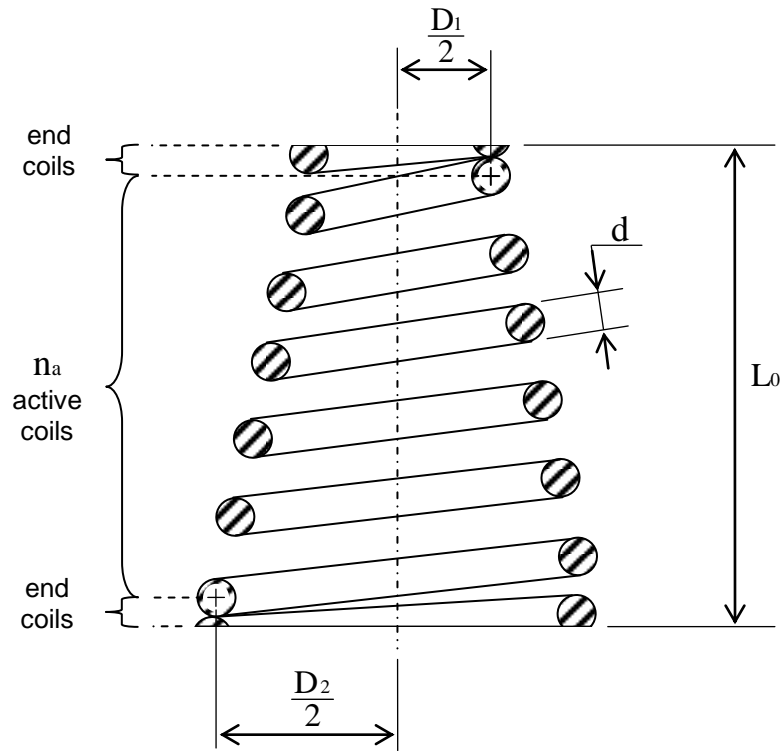


**Fig. 1 Parameters of the studied conical spring**

$n_a$  represents the active coils of the spring. In order to make the load as close as possible to an axial load, two end coils are added, with one at the top and one at the bottom of the spring. As for compression springs,  $n_i$  represents the difference between the overall length and the active length due to end coils.

Thus

$$L_a = L_0 - n_i d \quad (1)$$

$$L_c = L_s + n_i d \quad (2)$$

When end coils are correctly defined, they do not influence the behavior of the active coils. For this reason, the present work refers essentially to the active coils of the spring.

Spring behavior also depends on the shear modulus of elasticity  $G$  of the material.

**2.2 Two operating modes at minimum length.** At minimum length (i.e. maximum compression) and according to its initial geometry, the studied conical spring can adopt either of two types of coil arrangements (see Fig. 2):

- *type 1*: coils are solid, i.e. they are stacked one above the other, in contact coil-to-coil, giving a solid conical shape;
- *type 2*: the spring telescopes and the coils reach the ground, showing a flat spiral shape.

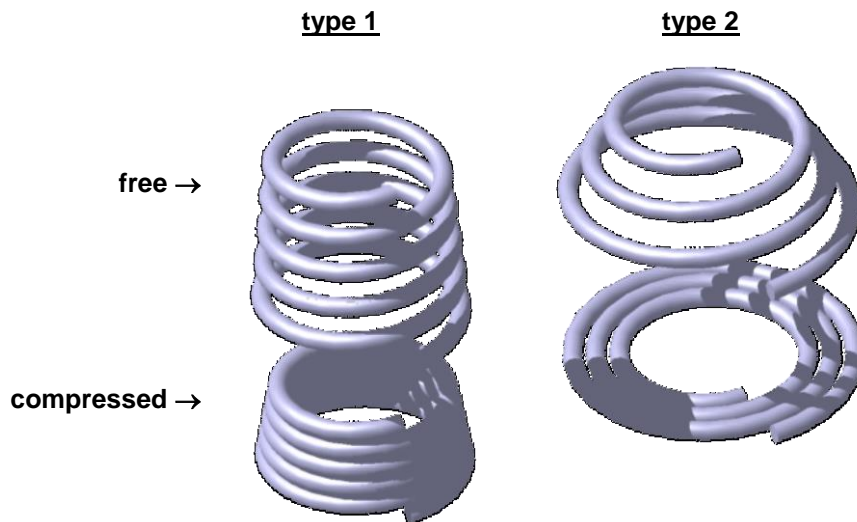


**Fig. 2 Active coil arrangements of type 1 and type 2 conical springs**

The criteria that distinguish telescoping springs (type 2) from non-telescoping ones (type 1) are geometrically determined (see Table 1).

The spring does not telescope (type 1) when  $n_a d > \frac{D_2 - D_1}{2}$ .

The spring telescopes (type 2) when  $n_a d \leq \frac{D_2 - D_1}{2}$ .

Both these types will be taken into account for the following calculations.

**2.3 Behavior law.** Constant pitch conical springs show a 2-phase compression in relation to their load-length characteristics (see Fig. 3): the first phase is linear (with a straight slope, as with a basic cylindrical spring), and the second phase is non-linear (at the end of compression).

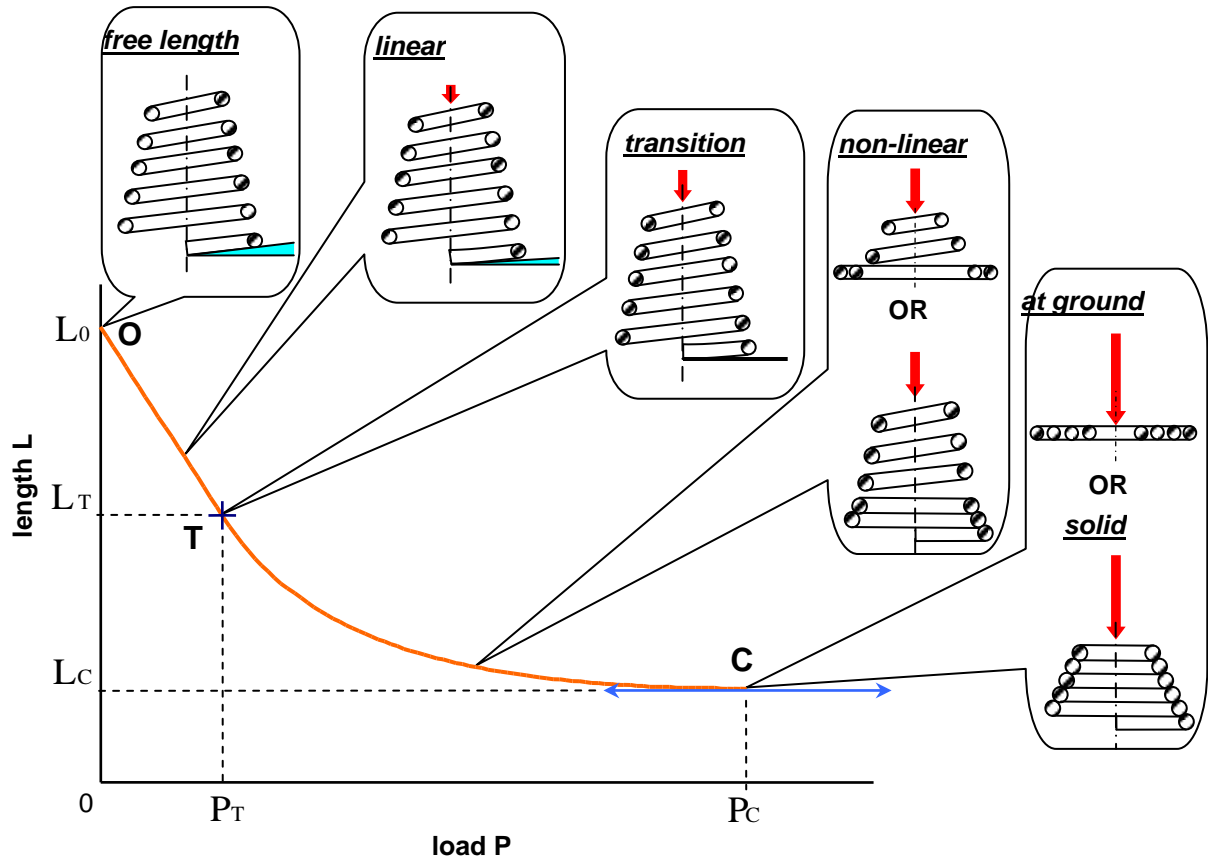


**Fig. 3 Deflection curve and successive coil arrangements according to compression phases**

(only active coils are displayed)

**2.4 Location of characteristic points O, T and C.** Three particular points of the load-length curve (see Fig. 3) can be defined to delimit linear and non-linear phases. The first point O corresponds to the free state of the spring, i.e. the initial stage of compression where  $P=0$  and  $L = L_0$ . The second point T represents the transition between both the above mentioned phases. The third point C marks the maximum compression state when spring length  $L$  cannot be shorter.

As the first stage of our analytical study of conical springs, the precise determination of points T and C locations is proposed, with the O point location already being known. Consequently, analysis of the compression process is needed to link these particular points to the spring's inherent physical behavior, and then to its parameters.

**2.4.1 Compression process analysis.** In the linear phase [OT] of the deflection curve (see Fig. 3), all the  $n_a$  active coils are free to deflect, and the spring rate is constant [11]:

$$R = \frac{G d^4}{2 n_a (D_1^2 + D_2^2) (D_1 + D_2)} \quad (3)$$

Along the non-linear phase [TC] (see Fig. 4), the active coils gradually stack one above the other. During this phase,  $n_f$  coils are free and  $(n_a - n_f)$  coils are at solid/ground, i.e. either ‘at solid’ for a type 1 spring, or ‘at ground’ for a type 2 spring.  $n_f$  represents the number of coils that are still free to deflect.

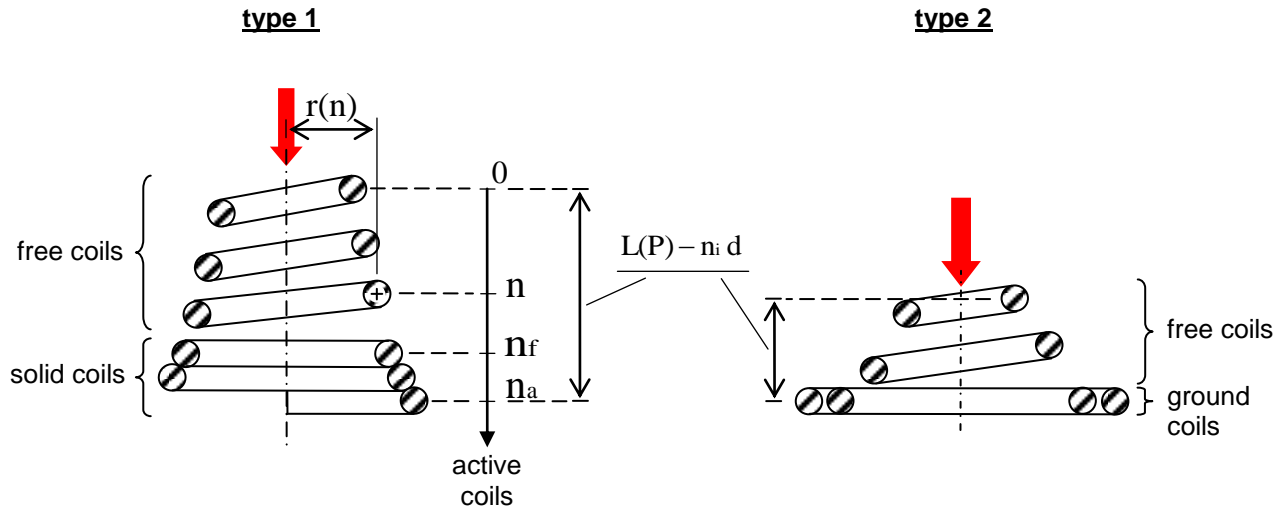


**Fig. 4 Distribution of active coils, at any step of the non-linear phase**

This physical behavior explains why the conical spring characteristic curve shows two different phases: linear and non-linear. In fact, in the linear phase between O and T, the first element of the largest coil is free and so deflects. All the  $n_a$  coils of the spring deflect so the spring rate  $R$  is constant and the load-length characteristic is linear. When the first element of the largest coil has reached its maximum physical deflection  $\delta_s$ , it ceases to be an active element of the spring since it is now ‘solid’ or ‘at ground’. This defines the point T. The first phase of compression now stops and the second one begins. Between T and C, the spring rate is then due to the ‘still free’  $n_f$  coils. During the second phase of compression,  $n_f$  continuously decreases from  $n_a$  to 0 and leads to a gradual increase in the spring rate. This explains why this second phase shows a non-linear load-length characteristic. Finally at the end of compression, the last free coil element with the smallest diameter  $D_1$  reaches its maximum deflection  $\delta_s$  and indeed defines the maximum load  $P_c$ . This analysis is a first step in determining points T and C, and then elaborating the method which will then be used to calculate the conical spring deflection. As a first result, this shows the role of the elementary coil deflections in determining these points. Secondly, analysis enables the active coil deflection of the entire spring to be divided into two components:

- deflection of the active coils of a first conical spring with  $n_f$  coils in its linear behavior,
- deflection of the active coils of a second conical spring with  $(n_a - n_f)$  coils at solid/ground.



2.4.2 *Definitions of elementary deflections.* For the linear behavior of a constant pitch conical spring, the elementary deflection of any part of coil marked  $n$  corresponds to the elementary deflection of free coils and can be calculated as for a basic cylindrical spring [1]:

$$\delta_f(n) = \frac{64 P [r(n)]^3}{G d^4} d n \quad (4)$$

where  $r(n) = \frac{1}{2} [D_1 + (D_2 - D_1)n/n_a]$  is the local mean coil radius described on Fig. 4.

Moreover, the elementary deflection at solid/ground corresponds to the maximum geometrical elementary deflection described in Table 1 and can be calculated as follows (whether the spring telescopes or not):

$$\delta_s = \frac{L_a - L_s}{n_a} d n \quad (5)$$

where 
$$L_s = \left\{ \max \left[ 0, (n_a d)^2 - \left( \frac{D_2 - D_1}{2} \right)^2 \right] \right\}^{1/2} \quad (6)$$

**Table 1** Lengths  $L_a$  and  $L_s$ , and associated phases of compression

	<u>free</u>	<u>any compression stage</u>	<u>at solid / at ground</u>
<b><u>type 1 springs</u></b>			
<b><u>type 2 springs</u></b>			

From these results and analysis, ‘transition point’ T and ‘maximum point’ C (cf. Fig. 3) can be obtained.

**2.4.3 Determination of ‘transition point’ T and ‘maximum point’ C.** On the conical spring load-length curve, the transition point T defines the connection between the linear phase (all active coils are free) and the non-linear phase (active coils gradually stack one above the other). T is defined by two values (its coordinates): the load at transition  $P_T$  and the length at transition  $L_T$ .  $P_T$  is the load for which the largest active coil ( $D_2$ ) reaches its maximum elementary deflection  $\delta_s$ . So at transition point T, this can be written:

$$\delta_f(D_2) = \delta_s$$

Thus

$$\frac{64 P_T (D_2/2)^3}{G d^4} = \frac{L_a - L_s}{n_a}$$

So

$$P_T = \frac{G d^4 (L_a - L_s)}{8 D_2^3 n_a} \quad (7)$$

Once  $P_T$  is known, length at transition is directly deduced:

$$L_T = L_0 - P_T/R \quad (8)$$

On the conical spring load-length curve, the maximum point C defines the ultimate compression state of the spring, i.e. the minimum length associated with the maximum load. C is defined by two values: the maximum load  $P_C$  and the minimum length  $L_C$ .  $P_C$  is the load for which the smallest active coil ( $D_1$ ) reaches its maximum elementary deflection  $\delta_s$ . So, analogically with the transition point above, this can be written:

$$P_C = \frac{G d^4 (L_a - L_s)}{8 D_1^3 n_a} \quad (9)$$

The associated length  $L_C$  can be calculated using Eq. (2). Points O, T and C have been completely defined and located on the load-length curve. The next step involves defining precise analytical expressions for the conical spring characteristics.

### 3 Length as a function of load

The object of this chapter is to define the analytical Length vs. Load expression for a constant pitch conical spring (see Fig. 3).

The most efficient method currently used for the Length vs. Load definition is proposed by IST [7]. The IST algorithm involves discretizing each coil of the conical spring into several angular parts. The deflection of the

spring for a given load is determined by adding the individual deflections of each part considered to be part of a cylindrical spring. Each individual deflection is limited to its maximum geometrical value. The expression  $\delta_f$  for these individual deflections and their limit  $\delta_s$  were determined in Section 2.4.2. The method introduced is based on the same principle as the IST algorithm, but where discretization is replaced by an integral approach. The determination steps of the analytical expression are presented below.

**3.1 Linear phase:**  $P \in [0; P_T]$ . During this phase, the spring rate  $R$  is constant so the length  $L$  associated with a load  $P$  can be easily calculated:

$$\text{For } P \in [0; P_T]: \quad L(P) = L_0 - P / R \quad (10)$$

**3.2 Non-linear phase:**  $P \in [P_T; P_C]$ . Spring length  $L$  is expressed from the spring overall free length  $L_0$  and its deflection  $\Delta$ :

$$L(P) = L_0 - \Delta \quad (11)$$

Analytical determination of the deflection  $\Delta$  is more direct than that for length  $L$ . Thus, the analytical expression of  $\Delta$  is proposed to lead on to the expression of  $L(P)$ .

At this stage,  $n_f$  (the number of current free coils) can be calculated as the value  $n$  for which elementary deflection of free coils reaches the elementary deflection at solid/ground for any load value  $P$  between  $P_T$  and  $P_C$ , i.e.:

$$\text{For } P \in [P_T; P_C]: \quad \delta_f(n_f) = \delta_s$$

$$\text{Thus} \quad \frac{64 P [r(n_f)]^3}{G d^4} = \frac{L_a - L_s}{n_a}$$

$$\text{So that,} \quad n_f = \frac{n_a}{D_2 - D_1} \left[ \left( \frac{(L_a - L_s) G d^4}{8 P n_a} \right)^{1/3} - D_1 \right] \quad (12)$$

Total spring deflection  $\Delta$  is the sum of both free coils and solid/ground coils deflections:

$$\Delta = \Delta_f + \Delta_s$$

$$\Delta = \int_0^{n_f} \delta_f(n) + \int_{n_f}^{n_a} \delta_s$$

$$\text{Finally: } \Delta(P) = \frac{2 P D_1^4 n_a}{G d^4 (D_2 - D_1)} \left[ \left( 1 + \left( \frac{D_2}{D_1} - 1 \right) \frac{n_f}{n_a} \right)^4 - 1 \right] + (L_a - L_s) \left( 1 - \frac{n_f}{n_a} \right) \quad (13)$$

*Note:* Once  $n_f$  is known, an alternative method, introduced in Appendix 1, can be used to determine  $\Delta_f$  and  $\Delta_s$ .

The length of a constant pitch conical spring (whether of type 1 or type 2) can thus be calculated using the following formula.

$$L(P) = L_0 - \left\{ \frac{2 P D_1^4 n_a}{G d^4 (D_2 - D_1)} \left[ \left( 1 + \left( \frac{D_2}{D_1} - 1 \right) \frac{n_f}{n_a} \right)^4 - 1 \right] + (L_a - L_s) \times \left( 1 - \frac{n_f}{n_a} \right) \right\} \quad (14)$$

With  $L_a$ ,  $L_s$  and  $n_f$  defined respectively in Eq. (1), (6) and (12).

**3.3 General equation.** From its definition,  $n_f$  exists whatever the compression load value  $P$ . But as compression begins, the load remains lower than  $P_T$  and all the active coils  $n_a$  are logically free, so  $n_f = n_a$  whatever the  $P$  value. Conversely, when compression comes to an end, the load becomes higher than  $P_s$  and logically there will be no remaining free coil, so  $n_f = 0$  whatever the  $P$  value. This implies two consequences relating to Eq. (12):

- If  $P < P_T$ , numerically  $n_f > n_a$ .
- If  $P > P_s$ , numerically  $n_f < 0$ .

For these reasons, numerical safeguards are proposed to be added to Eq. (12) so as to preclude inconsistencies such as  $n_f > n_a$  and  $n_f < 0$  while allowing for the use of the  $n_f$  analytical definition whatever the value of load  $P$ :

$$\text{For any } P: \quad n_f = \max \left\{ \min \left\{ \frac{n_a}{D_2 - D_1} \left[ \left( \frac{(L_a - L_s) G d^4}{8 P n_a} \right)^{1/3} - D_1 \right]; n_a \right\}; 0 \right\} \quad (15)$$

Combining Eq. (14) and Eq. (15) the length of the spring can be calculated without calculating  $P_C$  and  $P_T$ .

## 4 Load as a function of length

In the above,  $L(P)$  is proposed. This is an analytical expression of length as a function of load, for a constant pitch conical spring. Thus, for any load, the precise associated theoretical length is obtained. The inverse process (i.e. determination of load from any length value, see Fig. 5) would also be of interest for conical spring design and to predict the springs' behavior and characteristics.

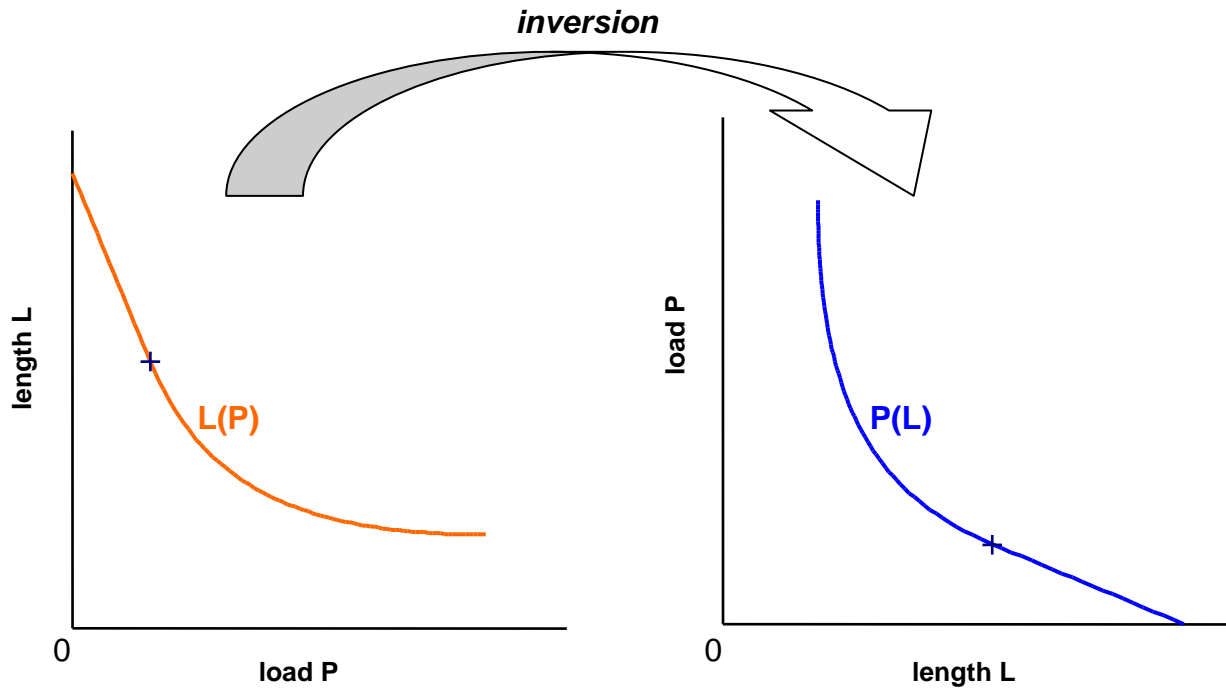


Fig. 5 Graphic representations of  $L(P)$  and its inverse  $P(L)$  for the same conical spring

For this reason, we propose in what follows to determine  $P(L)$ , an analytical expression of load as a function of length, for a constant pitch conical spring. The expression  $P(L)$  is studied and defined for two separate domains: the linear phase, and the non-linear phase (see Fig. 6). T and C coordinates are described in Section 2.4.3.

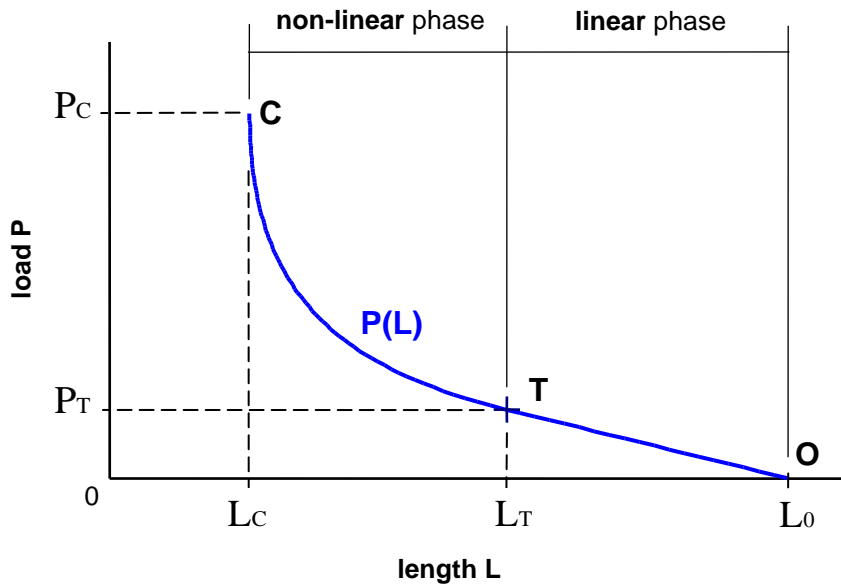


Fig. 6  $P(L)$  domains of definition (linear and non-linear)

#### 4.1 Linear phase. $L \in ]L_T; L_0]$

Here, spring rate  $R$  is constant, so  $L(P)$  is easy to inverse into  $P(L)$ :

$$\text{For } L \in ]L_T; L_0]: \quad P(L) = R(L_0 - L) \quad (16)$$

#### 4.2 Non-linear phase. $L \in [L_S; L_T]$

Here, the spring rate is no longer constant. To inverse  $L(P)$  and obtain  $P(L)$  for  $L \in [L_S; L_T]$ , the simplest way is to solve Eq. (13) where  $P$  becomes the unknown term and  $\Delta$  is a given value. Then, Eq. (13) can be changed into a polynomial equation of  $P^{1/3}$ , as shown below.

For  $L \in [L_S; L_T]$ , Eq. (13) can be developed as:

$$\begin{aligned} \Delta = (L_a - L_s) \frac{D_2}{D_2 - D_1} - \frac{1}{P^{1/3}} \left( \frac{G d^4}{8 n_a} \right)^{1/3} \frac{(L_a - L_s)^{4/3}}{D_2 - D_1} \\ + \frac{1}{P^{1/3}} \left( \frac{2 D_1^4 n_a}{G d^4 (D_2 - D_1)} \right) \left( \frac{(L_a - L_s) G d^4}{8 D_1^3 n_a} \right)^{4/3} - P \times \frac{2 D_1^4 n_a}{G d^4 (D_2 - D_1)} \end{aligned}$$

A simplified expression can be written as follows:

$$\Delta = K_7 + K_6 \times 1/P^{1/3} + K_5 \times P \quad (17)$$

$$\text{with: } \begin{cases} K_5 = -\frac{2 D_1^4 n_a}{G d^4 (D_2 - D_1)} & (18) \\ K_6 = -\frac{3}{8 (D_2 - D_1)} \left( \frac{G d^4 (L_a - L_s)^4}{n_a} \right)^{1/3} & (19) \\ K_7 = (L_a - L_s) \frac{D_2}{D_2 - D_1} & (20) \end{cases}$$

Then, Eq. (17) multiplied by  $P^{1/3}$  gives:

$$K_5 \times P^{4/3} + (K_7 - \Delta) P^{1/3} + K_6 = 0$$

And assuming  $x = P^{1/3}$ , a fourth order polynomial equation of  $x$  can be written in the conventional form:

$$x^4 + a_1 x + a_0 = 0$$

$$\text{with: } \begin{cases} a_1 = \frac{K_7 - \Delta}{K_5} = \frac{K_7 - L_0 + L}{K_5} \\ a_0 = K_6 / K_5 \end{cases}$$

Using a mathematical resolution of a fourth order polynomial, based on Cardan's method and detailed in Appendix 2, an analytical solution is found:

$$x = \left\{ \frac{1}{2} \left( b + \frac{a_0}{3b} \right) \right\}^{1/2} - \left\{ \frac{1}{2} \left( b + \frac{a_0}{3b} \right) - \left( b + \frac{a_0}{3b} - \left( \left( b + \frac{a_0}{3b} \right)^2 - a_0 \right)^{1/2} \right) \right\}^{1/2}$$

$$\text{with: } b = \left[ a_1^2/16 + \left( a_1^4/256 - a_0^3/27 \right)^{1/2} \right]^{1/3}$$

So a solution of Eq. (17) is obtained to give P(L), the analytical expression of load as a function of length for a constant pitch conical spring in its non-linear phase:

$$\text{For } L \in [L_s ; L_T]: \quad P(L) = (K_1/2)^{3/2} \left\{ 1 - \left( 1 - 2 \left[ 1 - \left( 1 + K_2/K_1^2 \right)^{1/2} \right] \right)^{1/2} \right\}^3 \quad (21)$$

$$\text{with: } \left\{ \begin{array}{l} K_1 = K_3 - \frac{K_2}{3K_3} \end{array} \right. \quad (22)$$

$$K_2 = -K_6/K_5 \quad (23)$$

$$K_3 = \left\{ K_4/16 + \left[ (K_4/16)^2 + (K_2/3)^3 \right]^{1/2} \right\}^{1/3} \quad (24)$$

$$K_4 = \left( \frac{K_7 - L_0 + L}{K_5} \right)^2 \quad (25)$$

$K_5, K_6$  and  $K_7$  being defined respectively in Eq. (18), (19) and (20)

## 5 Comparison with experimental data

The method presented is based on the principle of the IST algorithm but where discretization is replaced by an integral approach. Thus, the proposed analytical formulas perfectly fit the results of the IST algorithm [7] when the spring is highly discretized.

In order to validate the new conical spring models presented above, experimental tests were conducted. Telescoping and non-telescoping springs were tested. Load-length characteristics were measured for several constant pitch conical springs and compared with the proposed models. The experimental process involved reading the spring overall length for several load levels during a compression phase. Figure 7 shows the results for a telescoping spring (#1) and a non-telescoping spring (#2). The geometry of both springs and data used to build these models are detailed in Table 2.

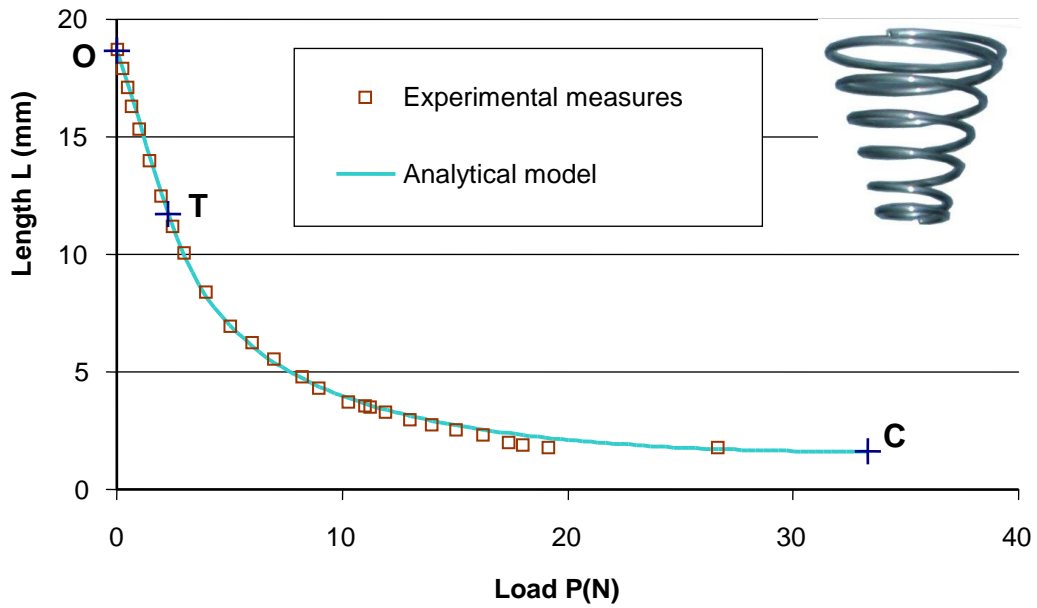
**Table 2 Characteristics of both conical springs #1 and #2**

	Spring #1	Spring #2
$D_1$	7.420 mm <i>0.2921 in</i>	8.970 mm <i>0.353 in</i>
$D_2$	18.30 mm <i>0.7205 in</i>	13.30 mm <i>0.5236 in</i>
$d$	0.8000 mm <i>0.03150 in</i>	1.200 mm <i>0.04724 in</i>
$L_0$	18.70 mm <i>0.7362 in</i>	37.20 mm <i>1.465 in</i>
$n_a$	4.5 coils	7.13 coils
$n_i$	2	1.5
$G$	72000 Mpa <i>10440000 psi</i>	80000 MPa <i>11600000 psi</i>

These results clearly show correct correlation between the analytical models and real spring behavior.



**#1 - Telescoping conical spring**



**#2 - Non-telescoping conical spring**

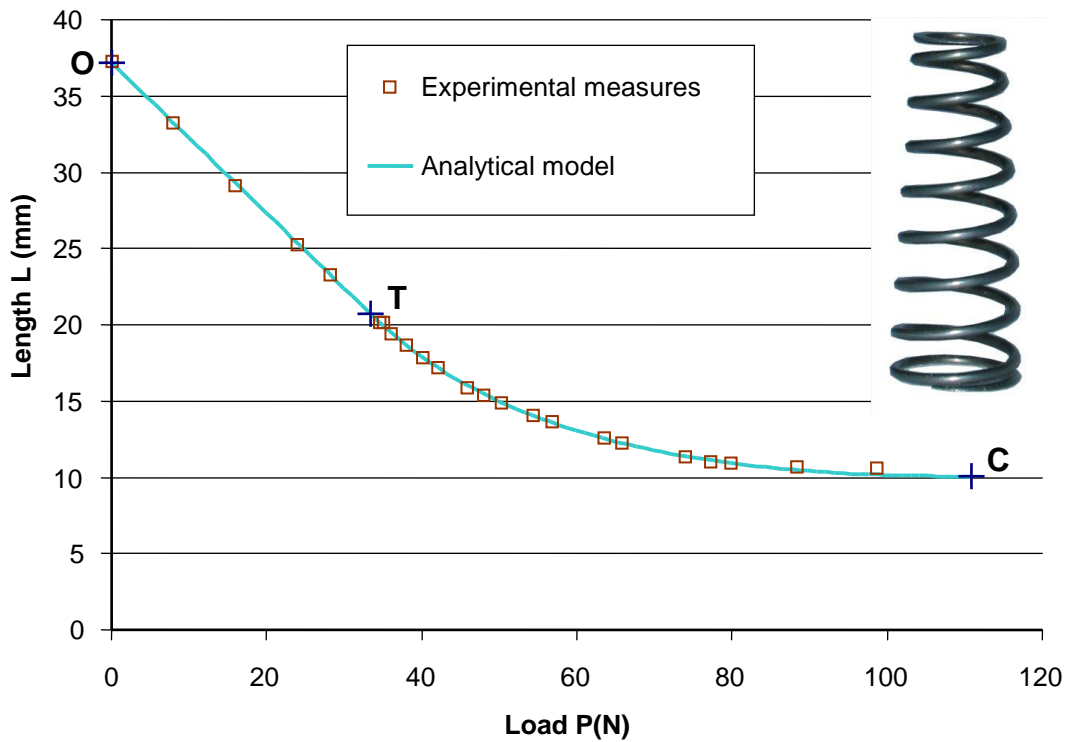


**Fig. 7 Experimental data and analytical model of two constant pitch conical springs, #1 is telescoping, #2 is non-telescoping**

## 6 Application of the proposed conical spring models

An application is submitted to show the efficiency of the proposed conical spring models. For a sensor mock-up development, a designer needs a conical spring that telescopes, provides a first operating point with a 10 N (2.248 lbf) load, and accepts a 6 mm (0.2362 in) spring travel defining a second operating point for which the load has to remain between 19 N and 21 N (4.271 lbf and 4.721 lbf), as described in Fig. 8. The designer has two telescoping springs that appear to be correct according to a first dimensional approach. These springs then have to be evaluated precisely, i.e. determination for each spring of its length  $L_1$  for the first operating point and of the resulting load  $P_2$  for the second point, to conclude as to whether at least one of the springs is of interest. The spring parameters are shown in Table 3.

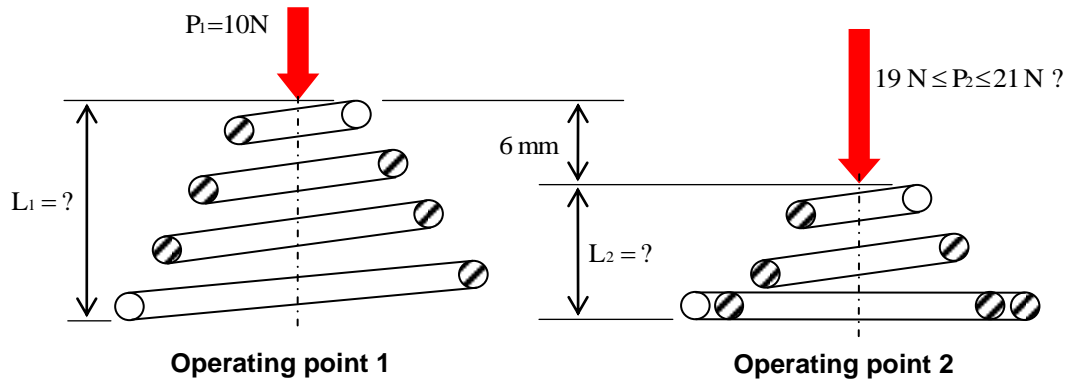


Fig. 8 Both operating points needed for conical springs #3 and #4

Table 3 Parameters of springs #3 and #4

	Spring #3	Spring #4
$D_1$	10.00 mm <i>0.3937 in</i>	8.000 mm <i>0.3150 in</i>
$D_2$	20.00 mm <i>0.7874 in</i>	23.00 mm <i>0.9055 in</i>
$d$	1.000 mm <i>0.03937 in</i>	1.000 mm <i>0.03937 in</i>
$L_0$	25.00 mm <i>0.9843 in</i>	35.00 mm <i>1.378 in</i>
$n_a$	3.5 coils	7 coils
$n_i$	1	1
$G$	80000 Mpa <i>11600000 psi</i>	80000 MPa <i>11600000 psi</i>

**6.1 Calculation of the first operating lengths  $L_1$ .** The conical spring parameters and the first operating load  $P_1$  are known. The corresponding spring lengths  $L_1$  can thus be evaluated using the proposed model for both springs. The generalized equation for  $n_f$  defined by Eq. (15) means Eq. (14) can be used to calculate  $L_1$  directly whether the spring is in its linear range or in its non-linear range. Results are shown in Table 4.

**Table 4 Calculation of  $L_1$  with  $P_1=10\text{ N}$  for springs #3 and #4**

	Spring #3	Spring #4	see
$L_a$	24.00 mm <i>0.9449 in</i>	24.00 mm <i>0.9449 in</i>	Eq. (1)
$L_s$	0.000 mm <i>0.000 in</i>	0.000 mm <i>0.000 in</i>	Eq. (6)
$n_f$	3.149 coils	4.170 coils	Eq. (15)
$L_1$	12.07 mm <i>0.4752 in</i>	12.13 mm <i>0.4776 in</i>	Eq. (14)

**6.2 Calculation of the second operating loads  $P_2$ .** The second operating lengths  $L_2$  (deduced from  $L_1$  and spring travel of 6 mm) are known. The corresponding spring loads  $P_2$  can thus easily be evaluated by the proposed model, to verify whether they are between 19 N and 21 N or not.

The model proposed to evaluate the spring load from any length is divided into two parts: Eq. (16) for a length in the linear phase and Eq. (21) for a length in the non-linear phase. First, the length at transition  $L_T$  is to be evaluated to determine to which phase  $L_2$  belongs.  $L_T$  is calculated using Eq. (8). For both tested springs  $L_2 \leq L_T$ ,  $L_2$  thus belongs to the non-linear phase and  $P_2$  is evaluated with Eq. (21). The results are shown in Table 5.

**Table 5 Calculation of  $P_2$  from  $L_2$  for springs #3 and #4**

	Spring #3	Spring #4	see
$L_2$	6.07 mm <i>0.2390 in</i>	6.13 mm <i>0.2413 in</i>	
$L_T$	13.75 mm <i>0.5413 in</i>	22.20 mm <i>0.8740 in</i>	Eq. (8)
$P_2$	19.51 N <i>4.386 in</i>	21.72 N <i>4.883 in</i>	Eq. (21)

**6.3 Selection of the appropriate spring.** Table 5 shows that only spring #3 matches the requirements relating to  $P_2$ . It is thus retained for design of the sensor mock-up.

## 7 Conclusion

This paper presents two models for determining the behavior of a constant pitch conical spring. They were developed to improve currently available conical spring design software. The proposed models involve two analytical equations, with the first giving spring length as a function of load and the second being the exact inverse by giving load as a function of length. Moreover, the length expression is proved to be written as a polynomial. The new models were successfully confronted with experimental data and an example of an application was presented.

The results of this study provide a very fast and precise calculation process. Using it, designers will be able to obtain any conical spring characteristic simply using a single formula (or just two formulas if the inverse calculation is needed), avoiding painstaking algorithm programming. In answer to our requirement to use load-length relations, the new models will pave the way for the development of a conical spring design synthesis tool based on optimization methods.

## Acknowledgments

The authors would like to thank Schneider Electric Industries and especially A. Samperio for his support to this research project and the Institute of Spring Technology for the highly relevant advice of J. Desforges and J.E. Slade.

## Nomenclature

- D = Local mean diameter of coil, mm
- $D_1$  = Mean diameter of the smallest active coil, mm
- $D_2$  = Mean diameter of the largest active coil, mm
- G = Shear modulus of elasticity, MPa
- L = Overall length (compression phase), mm
- $L_C$  = Overall solid length, mm
- $L_S$  = Solid length of active coils (between wire sections central points), mm

- $L_T$  = Overall length at transition point, mm  
 $L_a$  = Initial active length (between wire sections central points), mm  
 $L_0$  = Free length, mm  
 $L_1$  = First operating length, mm  
 $L_2$  = Second operating length, mm  
 $P$  = Load, N  
 $P_C$  = Maximum load, N  
 $P_T$  = Transition load (between linear and non-linear behavior), N  
 $P_1$  = First operating load, N  
 $P_2$  = Second operating load, N  
 $R$  = Constant spring rate (linear behavior), N/mm  
 $d$  = Wire diameter, mm  
 $n$  = Number of coils, as a continue variable running from 0 (at  $D_1$ ) to  $n_a$  (at  $D_2$ )  
 $n_a$  = Total number of active coils  
 $n_f$  = Number of free coils (variable during the compression phase)  
 $n_i$  = Parameter defining the influence of end coils on the difference between  $L_0$  and  $L_a$   
 $r$  = Local mean radius of coil, mm  
 $\Delta$  = Total deflection, mm  
 $\Delta_f$  = Deflection of free coils, mm  
 $\Delta_s$  = Deflection of solid coils (or ground coils), mm  
 $\delta_f$  = Elementary deflection of free coils, mm  
 $\delta_s$  = Elementary deflection of solid coils (or ground coils), mm

## Appendix 1

### Second method to obtain $\Delta_f$ and $\Delta_s$ .

If  $n_f$  is known, another method – with no integration process – can be used to determine  $\Delta_f$  and  $\Delta_s$ .

**Deflection of free coils.**  $\Delta_f$  corresponds to the deflection in the linear phase of a virtual conical spring for which active coils would be only those coils currently free. The characteristics of this virtual spring depend on  $P$ .

Its largest coil diameter  $D$  corresponds to the original spring's ' $n_f^{\text{th}}$ ' coil:

$$D = 2 r(n_f) = D_1 + (D_2 - D_1) n_f / n_a \quad (26)$$

Its rate R is deduced:

$$R = \frac{G d^4}{2 n_f (D_1^2 + D_2^2) (D_1 + D_2)} \quad (27)$$

Therefore its deflection gives directly  $\Delta_f$  :

$$\Delta_f = P/R \quad (28)$$

This can be developed as:

$$\Delta_f = \frac{2 P D_1^4 n_a}{G d^4 (D_2 - D_1)} \left[ \left( 1 + \left( \frac{D_2}{D_1} - 1 \right) \frac{n_f}{n_a} \right)^4 - 1 \right] \quad (29)$$

**Deflection of solid/ground coils.**  $\Delta_s$  is the part of the maximum deflection corresponding to the solid/ground coils (( $n_a - n_f$ ) coils). Since the maximum deflection is geometrically the difference between the initial active length  $L_a$  and the solid length of active coils  $L_s$ ,  $\Delta_s$  can be directly obtained as:

$$\Delta_s = (L_a - L_s) \times \frac{n_a - n_f}{n_a} = (L_a - L_s) \times (1 - n_f/n_a) \quad (30)$$

## Appendix 2

### Resolution of fourth order polynomial equations (Cardan's method).

#### Fourth order polynomial

Starting from equation:  $x^4 + a.x^3 + b.x^2 + c.x + d = 0$ .

Change of variable:  $x = z - a/4$ .

The following equation is then obtained:  $z^4 + p.z^2 + q.z + r = 0$ .

$$\text{With: } \begin{cases} p = b - 3a^2/8 \\ q = c - a.b/2 + a^3/8 \\ r = d - a.c/4 + b.a^2/16 - 3a^4/256 \end{cases}$$

For the equation in Z, two cases may occur: (i)  $q = 0$  and (ii)  $q \neq 0$ .

(i)  $q = 0$ . The equation is then:  $z^4 + p.z^2 + r = 0$ .

Assuming  $y = z^2$ , the equation becomes  $y^2 + p.y + r = 0$ .

Solutions are as follows:

$$y_1 = -p/2 + (p^2/4 - r)^{1/2} \quad \text{and} \quad y_2 = -p/2 - (p^2/4 - r)^{1/2}$$

Hence:  $z_1 = y_1^{1/2}$ ;  $z_2 = -y_1^{1/2}$ ;  $z_3 = y_2^{1/2}$  and  $z_4 = -y_2^{1/2}$ .

(ii)  $q \neq 0$ . The equation is then:  $z^4 + p.z^2 + q.z + r = 0$ .

Assuming:  $2P - Q^2 = p$ ;  $-2Q.R = q$  and  $P^2 - R^2 = r$ .

This reduced equation is obtained:  $(z^2 + P)^2 - (Q.z + R)^2 = 0$ .

$$[\text{another form of } z^4 + p.z^2 + q.z + r = 0]$$

$P$ ,  $Q$  and  $R$  have to be found, solving this system:

$$\begin{cases} 2P - Q^2 = p \\ -2Q.R = q \\ P^2 - R^2 = r \end{cases} \quad [\text{S}]$$

Equivalent to:

$$\begin{cases} Q^2 = \frac{q^2}{4(P^2 - r)} \\ R^2 = P^2 - r \\ Q.R = -q/2 \end{cases}$$

[S] can be converted in this third order polynomial equation (in  $P$ ):

$$P^3 - p.P^2/2 - r.P + p.r/2 - q^2/8 = 0$$

Then a solution  $P_0$  is obtained (see hereafter the paragraph "Third order polynomial").

Via [S], a couple  $(Q_0, R_0)$  is associated with  $P_0$ .

Then solutions of the reduced equation are solutions of:

$$\begin{cases} z^2 + P_0 + Q_0.z + R_0 = 0 \text{ or} \\ z^2 + P_0 - Q_0.z - R_0 = 0 \end{cases}$$

Finally,  $z$  is obtained.

### Third order polynomial

Starting from equation:  $x^4 + a.x^3 + b.x^2 + c.x + d = 0$ .

Change of variable:  $x = z - a/3$ .

Then the following equation is obtained:  $z^3 + p.z + q = 0$ .

$$\text{With: } \begin{cases} p = b - a^2/3 & \text{and} \\ q = 2a^3/27 - a.b/3 + c \end{cases}$$

Note:

Once a solution  $z_0$  of the equation in  $z$  is obtained, then:

$x_0 = z_0 - a/3$  is a solution of the equation in  $x$ .

For the equation in  $z$ , two cases may occur: (i)  $p = 0$  and (ii)  $p \neq 0$ .

(i)  $p = 0$ . The equation becomes  $z^3 = -q$ .

This equation has three solutions in  $\mathbf{C}$  :

$$\begin{cases} z_1 = (-q)^{1/3} \\ z_2 = j.z_1 \\ z_3 = j^2.z_1 \end{cases}$$

$$\text{Where } j = \frac{-1 + i\sqrt{3}}{2}$$

(ii)  $p \neq 0$ . The equation is  $z^3 + p.z + q = 0$ .

Another change of variable:  $z = u + v$ . With  $u \neq 0$ .

The equation then becomes:

$$u^3 + v^3 + q + (3u.v + p)(u + v) = 0$$



This system is then considered:

$$\begin{cases} u^3 + v^3 + q = 0 & [S] \\ 3u.v + p = 0 \end{cases}$$

The [S] system is equivalent to:

$$\begin{cases} u^6 + q.u^3 - \frac{p^3}{27} = 0 \\ v = \frac{-p}{3u} \end{cases}$$

Change of variable in the first equation:  $y = u^3$

The equation becomes:  $y^2 + q.y - p^3/27 = 0$

Therefore a solution is:

$$y = -q/2 + (q^2/4 + p^3/27)^{1/2}$$

Then, solutions of  $y = u^3$  are to be found (cf case(i) ). Here then are the solutions:

$$\begin{cases} u_1 = y^{1/3} & \text{and} & v_1 = \frac{-p}{3u_1} \\ u_2 = j.u_1 & \text{and} & v_2 = j.v_1 \\ u_3 = j^2.u_1 & \text{and} & v_3 = j^2.v_1 \end{cases}$$

Hence  $Z_1 = u_1 + v_1$ ,  $Z_2 = u_2 + v_2$  and  $Z_3 = u_3 + v_3$ .

Which leads to solutions for  $X$ .

## References

- [1] Wahl, A. M., 1963, *Mechanical Springs*, McGraw-Hill Book Company, New York.
- [2] Ding, X, and Selig, J.M., 2004, "On the Compliance of Coiled Springs," *International Journal of Mechanical Sciences*, **46**, pp. 703-727.
- [3] Chassie, G.G., Becker, L.E., and Cleghorn, W.L., 1997, "On the Buckling of Helical Springs Under Combined Compression and Torsion," *International Journal of Mechanical Sciences*, **39**(6), pp. 697-704.
- [4] Becker, L.E., Chassie, G.G., and Cleghorn, W.L., 2002, "On the Natural Frequencies of Helical Compression Springs," *International Journal of Mechanical Sciences*, **44**, pp. 825-841.
- [5] Jiang, W.G., and Henshall, J.L., 2000, "A Novel Finite Element Model for Helical Springs," *Finite Elements in Analysis and Design*, **35**, pp. 363-377.

- [6] Todinov, M.T., 1999, "Maximum Principal Tensile Stress and Fatigue Crack Origin for Compression Springs," *International Journal of Mechanical Sciences*, **41**, pp. 357-370.
- [7] IST, 1980 - 2005, "Essential Spring Design Training Course," handbook, The Institute of Spring Technology, Sheffield, United Kingdom.
- [8] Wolansky, E. B., 1995, "Fundamental Frequency," *Springs*, September, pp. 61-66.
- [9] Yildirim, V., 2002, "Expressions for Predicting Fundamental Natural Frequencies of Non-Cylindrical Helical Springs," *ASME Journal of Sound and Vibration*, **252**(3), pp. 479-491.
- [10] Yildirim, V., 2004, "A Parametric Study on Natural Frequencies of Unidirectional Composite Conical Spring," *Communications in Numerical Methods in Engineering*, **20**, pp. 207-227.
- [11] Wolansky, E. B., 1996, "Conical Spring Buckling Deflection," *Springs*, Winter, pp. 63-68.
- [12] Wolansky, E. B., 2001, "Lateral Loading of Conical Springs," *Springs*, April, pp. 95-98.
- [13] Spring Manufacturers Institute, Inc., 2001 Midwest Road, Suite 106, Oak Brook, Illinois 60523-1335 USA, [www.smihq.org](http://www.smihq.org)
- [14] Universal Technical Systems, Inc., 202 West State Street, Suite 700, Rockford, IL 61101 USA, [www.uts.com](http://www.uts.com)
- [15] The Institute of Spring Technology, Henry Street, Sheffield. S3 7EQ. UK., United Kingdom, [www.ist.org.uk/index.html](http://www.ist.org.uk/index.html)
- [16] Yoshimura, M., Nishiwaki, S., and Izui, K., 2005, "A Multiple Cross-Sectional Shape Optimization Method for Automotive Body Frames," *ASME Journal of Mechanical Design*, **127**(1), pp. 49-57.
- [17] Lyu, N., and Saitou, K., 2005, "Topology Optimization of Multicomponent Beam Structure via Decomposition-Based Assembly Synthesis," *ASME Journal of Mechanical Design*, **127**(2), pp. 170-183.
- [18] Giassi, A., Bennis, F., and Maisonneuve, J.-J., 2004, "Multi-Objective Optimization Using Asynchronous Distributed Applications," *ASME Journal of Mechanical Design*, **126**(5), pp. 767-774.
- [19] Maddisetty, H., and Frecker, M., 2004, "Dynamic Topology Optimization of Compliant Mechanisms and Piezoceramic Actuators," *ASME Journal of Mechanical Design*, **126**(6), pp. 975-983.
- [20] Sandgren, E., 1990, "Nonlinear Integer and Discrete Programming in Mechanical Design Optimization," *ASME Journal of Mechanical Design*, **112**(2), pp. 223-229.
- [21] Paredes, M., Sartor, M., and Masclet, C., 2002, "Obtaining an Optimal Compression Spring Design Directly From a User Specification," *Journal of Engineering Manufacture Part B, Proceedings of The Institution of Mechanical Engineers*, **216**, pp. 419-428.
- [22] Paredes, M., Sartor, M., and Masclet, C., 2001, "An Optimization Process for Extension Spring Design," *Computer Methods in Applied Mechanics and Engineering*, **191**, pp. 783-797.
- [23] Wu, M. H., and Hsu, W. Y., 1998, "Modelling the Static and Dynamic Behavior of a Conical Spring by Considering the Coil Close and Damping Effects," *ASME Journal of Sound and Vibration*, **214**(1), pp. 17-28.

## List of Figures

Fig. 1 Parameters of the studied conical spring

Fig. 2 Active coil arrangements for type 1 and type 2 conical springs

Fig. 3 Deflection curve and successive coil arrangements according to compression phases (only active coils are displayed)

Fig. 4 Distribution of active coils, at any step of the non-linear phase

Fig. 5 Graphic representations of  $L(P)$  and its inverse  $P(L)$  for the same conical spring

Fig. 6  $P(L)$  domains of definition (linear and non-linear)

Fig. 7 Experimental data and analytical model of two constant pitch conical springs, #1 is telescoping, #2 is non-telescoping

Fig. 8 Both the operating points needed for the conical springs #3 and #4

## List of Tables

Table 1 Lengths  $L_a$  and  $L_s$ , and associated phases of compression

Table 2 Characteristics of both conical springs #1 and #2

Table 3 Parameters of the springs #3 and #4

Table 4 Calculation of  $L_1$  with  $P_1 = 10 \text{ N}$  for springs #3 and #4

Table 5 Calculation of  $P_2$  from  $L_2$  for springs #3 and #4